Advances in Science and Technology Research Journal

Advances in Science and Technology Research Journal, 2026, 20(4), 35–44
https://doi.org/10.12913/22998624/213703
ISSN 2299-8624, License CC-BY 4.0

Received: 2025.09.13
Accepted: 2026.02.15
Published: 2026.03.01

Novel hybrid radial basis functions for the numerical analysis of anisotropic plate

Vivek G. Patel[1], Nikunj V. Rachchh[1*], Raghvendra Kumar Mishra[2]

[1] Department of Mechanical Engineering, Marwadi University, Rajkot, 360003, Gujarat, India
[2] Department of Mechanical Engineering, Shri Mata Vaishno Devi University, Sub-Post-Office, Katra, Jammu and Kashmir, 182320, India
* Corresponding author's email: nikunj.rachchh@marwadieducation.edu.in

ABSTRACT

Anisotropic plates are mainly used in advanced engineering applications because of their direction-dependent strength and light weight; nevertheless, their analysis is highly challenging because of its complex structure, varying loading and boundary conditions. The presented article proposed a novel hybrid radial basis function (H-RBF) method, which effectively combines multi-quadric (MQ) and thin plate spline (TPS) functions for the analysis of anisotropic plate. For the validation of the proposed technique, the Galerkin Method, ANSYS simulations, and conventional analytical models were employed. The reliability and validity of the H-RBF method were demonstrated using parametric simulation under different stiffness ratios, aspect ratios, and boundary conditions. Outcomes reflect displacement behaviour according to anisotropy variations with high correlation with classical solutions and benchmark solutions. H-RBF method was presented as a powerful and efficient alternative approach for anisotropic plate analysis in a wide range of problems.

Keywords: hybrid radial basis function method, MQ-RBF, TPS, anisotropic plate, meshless method.

INTRODUCTION

Anisotropic plates are gaining substantial importance in the majority of fields of engineering, especially in aerospace, defence, automotive, civil engineering, and materials science. Their higher mechanical properties and the ability to customise directional properties make them extremely useful for application in advanced composite laminates [1]. However, their inherent material properties of anisotropy, generally accompanied by complex geometries and nonlinear boundary conditions, the analysis of these structural components extremely difficult [2,3]. Accurate prediction of their mechanical behaviour under various loading conditions is a major hindrance for researchers in the field [4].

The widespread use of anisotropic plates in important engineering applications emphasises the need for precise and efficient analytical methods and encourages further research in finding robust methods [2]. Analytical solutions will often be insufficient due to complexities such as shape, type of the material and boundary conditions [5]. Over the last few decades, different methods have been explored by various researchers to overcome the challenges presented with analytical approaches. The finite element method (FEM) emerged as a valuable analysis tool that can solve many engineering problems; however, it too has several limitations [6–8]. Recent studies have shown that meshless methods, particularly radial basis function (RBF), offer a powerful solution as they do not depend on mesh and have numerical stability for anisotropic material and irregular geometries [9–11]. Meshless methods have also been used in the cases like elastostatic and the fractional-order PDEs, which demonstrates several advantages that extend across applications [9, 10]. The increasing need for improved analytical techniques will further drive the development of new computational

methods. These methods aim to remove mesh dependencies and improve meshless methods. This is done by combining different meshless method to develop novel hybrid method that work better for anisotropic and non-linear problems.

Background

Analysis of anisotropic plates presents inherent challenges due to the directional dependence of their material properties and the orientation of reinforcing fibres. Conventional finite element methods often encounter limitations in accurately modelling and meshing such anisotropic geometries, particularly when addressing complex geometries [12]. RBF techniques, on the other hand, gained the attraction of researchers, as it provides a meshless solution that makes use of distance-based interpolation and distributed nodal points. They work especially well with complicated geometries, anisotropic materials, and nonlinear behaviour [13,14]. A few recent articles highlighted the potency of RBF-based models in plate and shell mechanics, for example, the nonlinear laminated composite plate analysis using RBF-pseudospectral formulations [15] and shallow-shell based layerwise collocation theories [16].

The basic idea in RBF techniques is the use of combinations of radially symmetric basis functions in nodal points to compute an approximate displacement. This distance-dependent formulation is naturally well-adapted to irregular node distributions and can be generalised to anisotropic conditions by directional scaling. Among other RBF methods, multi-quadric RBF (MQ-RBF) is highly accurate for smooth solutions but highly sensitive to its shape parameters. For the purpose of addressing MQ shape-parameter issues, new hybrid kernel expressions such as the power-generalised MQ [17] and free-parameter MQ-based collocation formulations [18] have emerged, with reduced shape parameter dependency and improved conditioning. Similarly, local and h-adaptive RBF finite-difference (RBF-FD) formulations have made their appearance in order to overcome the issue of geometrical scales and stress regions that are spatially localised in elasticity applications [19]. For plate and beam structures, MQ-RBF formulations have been applied in nonlinear bending and composite modelling studies, validating their accuracy and efficiency [20, 21].

Modified space-time RBF collocation schemes have also been developed to improve long-time stability for transient heat conduction in anisotropic composite materials, underscoring their suitability for time-dependent and directionally varying problems [11]. Advanced RBF method such as integrated and extended RBF meshless methods, have further been applied to plate crack analysis, highlighting the adaptability of RBFs to structural discontinuities [22].

On the other hand, TPS is derived from the physical analogy of bending a thin elastic plate, where the interpolating surface minimises the bending energy. This characteristic makes TPS particularly suitable for problems involving plate deflections and curvature analysis. Due to its parameter-free nature, TPS provides ease-of-use during application; however, TPS can sometimes converging slower under some boundary conditions and lacks flexibility with complex geometries [23, 24]. In turn, MQ-RBF has greater accuracy and flexibility in some of those cases. Therefore, combining TPS and MQ-RBF in a hybrid scheme can be advantageous as well as leveraging the stability and smoothness of TPS with the precision and flexibility of MQ-RBF to achieve improved overall performance.

Notably, extensive surveys ratify that modern trends in RBF investigations rely heavily on hybridisation and adaptability to enhance accuracy and approximating performance in structure and composite studies [25]. To overcome individual limitations while maintaining strengths of both approaches, the current research was focused on establishing and validating a new H-RBF method by firm comparison with current numerical, analytical, and simulation approaches for anisotropic plates [26].

Novelty

The present research proposed a novel H-RBF based numerical method, intended to cater for the significant shortcomings of the widely used traditional FEM and RBF methodologies. The newly proposed H-RBF method introduces a new methodology by taking advantage of the benefits associated with MQ-RBF and TPS and combining their complementary features.

The H-RBF method is new in the sense that it inherits the high accuracy of MQ-RBF while making use of the good stability of the TPS, providing a balanced and efficient way to

approximate problems. Through such assimilation, the technique is stable for wide node distributions, irregular shapes, uniform as well as non-uniform grids, where mostly the FEM tend to fall short. Beyond that, H-RBF shows faster convergence and higher efficiency, while comparing with classical FEM and RBF methods in accuracy. The H-RBF method is advancement in the area of meshless numerical modelling, providing a useful and reliable tool for handling complex engineering and scientific problems that involve composite structures and other demanding areas.

THE CONSTRUCTION OF H-RBF

The H-RBF is created by combining the piecewise smooth TPS $\varphi_2(r)$ and infinitely smooth MQ-RBFs $\varphi_1(r)$. It can be expressed mathematically as Equation 1.

$$\varphi(r) = \varepsilon\varphi_1(r) + (1-\varepsilon)\varphi_2(r) \tag{1}$$

The weighting factor 'ε' is a natural number that regulates the contributions of each function in turn. While φ_1 is infinite smooth RBF having a user-specified 'c' shape parameter, $c \in N$; *and* φ_2 is piecewise smooth RBF that is independent of the shape parameter.

Mathematical representation

Multi-quadric radial basis function (MQ-RBF)

$$\varphi_{1j} = \sqrt{(x-x_j)^2 + (y-y_j)^2 + c^2} \tag{2}$$

Shape parameter, 'c' should be a user defined natural number.

The MQ-RBF method uses the radial function, as mentioned in Equation 2. The function is capable to achieve closer approximation and can achieve exponential convergence for smooth problems, making it suitable for the bending analysis of anisotropic plates [23]. Its meshless nature allows flexible node placement, which is valuable for irregular geometries and adaptive refinement.

A distinctive advantage of MQ-RBF in anisotropic plate analysis lies in its isotropic functional form, although the basis function itself is isotropic, anisotropy can be accounted by introducing scaling or transformation into the distance metric [14]. Moreover, MQ-RBF is effective in modelling nonlinear behaviours, which are often encountered in advanced plate models may include large deflection, post-buckling analysis, etc. [27].

However, MQ-RBF methods are sensitive to the shape parameter 'c'. An inappropriate choice can lead to ill-conditioned system matrices, affecting stability and accuracy. Additionally, due to their global support, MQ-RBFs result in dense matrices, making them computationally expensive for large-scale problems. The standard MQ also lacks polynomial consistency, although augmented versions can overcome this by including polynomial terms [24].

Thin plate spline (TPS)

$$\varphi_{2j} = \left((x-x_j)^2 + (y-y_j)^2\right)^{2\beta} \times \times ln((x-x_j)^2 + (y-y_j)^2) \tag{3}$$

2β is a positive integer number, and its value should be chosen by adding +1 value to the order of the governing equation used in MQ-RBF to avoid the issue that arises during the differentiation.

The TPS method is grounded in the physical analogy of bending a thin elastic plate and is based on the radial function Equation 3. Unlike MQ-RBF, TPS is independent of shape parameter, simplifying its application. TPS is having inherent characteristics of minimising bending energy in its formulation, making it an ideal choice for research focused on plate deflections and curvature associated with the analysis of anisotropic plates [23].

By using higher-order polynomial terms, TPS can produces smooth interpolating surfaces, and ensures polynomial consistency as it can accurately reproduce constant and linear fields, which is an important feature for reliable modelling of simple plate behaviour.

TPS has the ability to provide smooth interpolating surfaces with polynomial consistency through the use of higher-order polynomial terms that can exactly reproduce constants and linear fields, an essential property required for accurate simulations of the fundamental behaviour of plates.

Like MQ-RBF, TPS has global support, which leads to dense system matrices and potential ill-conditioning for larger data sets. In addition, the rigidity of the TPS basis function

does not provide the flexibility to capture more complicated or nonlinear behaviour of the plate.

A promising approach for the numerical solution of anisotropic plates is the hybridisation of both MQ-RBF and TPS methods, with each one mapping onto the strengths of the other method [27]. The MQ-RBF method is accurate, can be used for scattered data, and has excellent computational efficiency when approximating nonlinear and complex responses. Conversely, the TPS method ensures polynomial consistency, while also being parameter-free and simpler to implement. The combination of these two seemingly disparate methods leads to a hybrid RBF framework that balances flexibility and accuracy. MQ-RBF can be utilised as a solution for localized nonlinearities or complex boundary conditions and TPS for smoothness, consistency and energy [24]. This synergy of combination is able to overcome the limitations inherent in each method: TPS compensates for the sensitivity of MQ-RBF towards the change of shape parameters, while MQ-RBF compensates for the loss of flexibility that accompanies the use of a fixed functional form. Such a hybrid method is especially useful to anisotropic and non-smooth plate geometries, where stability and accuracy are more important. Further, it can lead to the solutions that are improved in stability, scalability, and physical consistency [14].

Governing equations of a thin plate

Figure 1 represents the geometry of a thin plate, dimensions, coordinate system and loading condition. Neglecting the rotary and in-plane inertia, the equation of anisotropic plate under uniform load can be expressed in non-dimensional form as Equation 4.

$$w_{xxxx} + 2\eta R^2 w_{xxyy} + \psi R^4 w_{yyyy} + \\ + 4R\,\varphi\, w_{xxxy} + 4\mu R^3 w_{xyyy} - q = 0 \tag{4}$$

Non-dimensional quantities can be defined as

$$w = w^*/h;\ x = x^*/a;\ y = y^*/b \\ R = a/b;\ \mathrm{t} = \mathrm{t}^*\sqrt{D_{11}/(\rho a^4 h)}; \\ \eta = (D_{12} + 2 * D_{66})/D_{11}; \\ \psi = D_{22}/D_{11};\ \varphi = D_{16}/D_{11}; \\ \mu = D_{26}/D_{11}$$

Governing equation

$$\sum_{j=1}^{N} w_j \frac{\partial^4}{\partial x^4}\varphi_j + 2\eta R^2 \sum_{j=1}^{N} w_j \frac{\partial^4}{\partial x^2 \partial y^2}\varphi_j + \\ + \psi R^4 \sum_{j=1}^{N} w_j \frac{\partial^4}{\partial y^4}\varphi_j + 4R\varphi \sum_{j=1}^{N} w_j \frac{\partial^4}{\partial x^3 \partial y}\varphi_j + \\ + 4\mu R^3 \sum_{j=1}^{N} w_j \frac{\partial^4}{\partial x \partial y^3}\varphi_j - q = 0 \tag{5}$$

Boundary conditions

Simple supported (S-S-S-S)

$$x = 0{,}1 \sum_{j=1}^{N} w_j\, \varphi_j = 0 \tag{6}$$

$$y = 0{,}1 \sum_{j=1}^{N} w_j\, \varphi_j = 0 \tag{7}$$

$$x = 0{,}1 \sum_{j=1}^{N} -D_{11} w_j \frac{\partial^2}{\partial x^2}\varphi_j - \\ - D_{12} R^2 w_j \frac{\partial^2}{\partial y^2}\varphi_j - 2D_{16} R\, w_j \frac{\partial^2}{\partial x \partial y}\varphi_j = 0 \tag{8}$$

$$y = 0{,}1 \sum_{j=1}^{N} -D_{12} w_j \frac{\partial^2}{\partial x^2}\varphi_j - \\ - D_{22} R^2 w_j \frac{\partial^2}{\partial y^2}\varphi_j - 2D_{26} R\, w_j \frac{\partial^2}{\partial x \partial y}\varphi_j = 0 \tag{9}$$

Clamped (C-C-C-C)

$$x = 0{,}1 \sum_{j=1}^{N} w_j\, \varphi_j = 0 \tag{10}$$

$$y = 0{,}1 \sum_{j=1}^{N} w_j\, \varphi_j = 0 \tag{11}$$

$$x = 0{,}1 \sum_{j=1}^{N} w_j \frac{\partial}{\partial x}\varphi_j = 0 \tag{12}$$

$$y = 0{,}1 \sum_{j=1}^{N} w_j \frac{\partial}{\partial y}\varphi_j = 0 \tag{13}$$

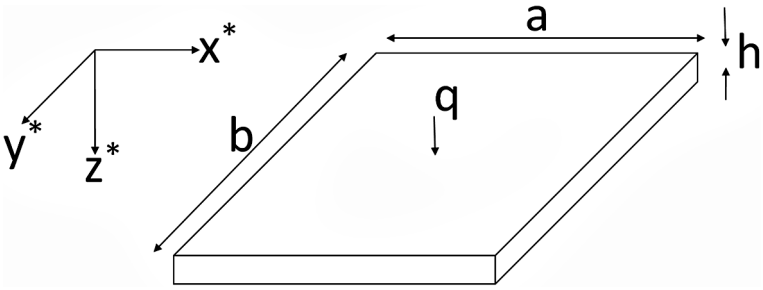

Figure 1. Geometry of a thin plate

In the present approach, the plate is divided into n × n points. Out of these (n-2) × (n-2) points are internal, while the remaining points lie at the boundaries. The governing equation Equation 5 generates $(n-2)^2$ equations for the internal collocation points. Additionally, each of the boundary conditions Equations 6–9 and Equations 10–13 contributes $2 \times (n^2-(n-2)^2) + 8$ equations, resulting in a total of $(n-2)^2 + 8n$ equations.

However, the total number of unknown weighing coefficients are n^2, lesser than the total number of equations. The imbalance leads to an ill-conditioned system. To address this issue, a multiple regression based approach using the least square method is employed.

The spatial domain is for independent variables $x \in [0,a]$ and $y \in [0,b]$. Dynamic terms are moved to the right side of the equation to maintain the invariability of the coefficient matrix and equation can be expressed as mentioned in Equation 14,

$$A \times a = q \tag{14}$$

where: A is $(l \times k)$ coefficient matrix, a is the (k×1) vector of unknown co-efficient and q is $(l \times 1)$ load vector representing governing as well as boundary conditions.

Minimising the residuals and obtain an approximation as in Equation 15, the regression gives,

$$a = (A^T A)^{-1} A^T P \tag{15}$$

where: $(A^T A)^{-1} A^T$ is the transformation matrix.

It effectively fits a hyper surface that satisfies the governing equation and boundary equations over the entire spatial domain, rather focusing on exact solution at each point. Consequently, the least-squares technique enhances numerical stability, reduces the consequence of over-specification, ensures consistency, and a viable solution.

RESULTS AND DISCUSSION

The effectiveness and robustness of the proposed H-RBF method were evaluated by analysing an anisotropic plate subjected to uniform transverse loading. For benchmarking purposes, the material is assumed to be homogeneous having uniform properties in all principal directions, allowing direct comparison with established analytical and numerical solutions. The study systematically investigated the response of plates with respect to different boundary conditions, aspect ratios, and anisotropy of material, then compared the findings with classical methods and recent computational techniques to verify the results.

Validation with existing benchmark methods

The proposed H-RBF method was validated against the classical analytical results derived by Timoshenko and Woinowsky-Krieger [28] as well as MATLAB code developed for well-established finite element formulation and the simulation results provided by ANSYS 2022 workbench.

For the FEM analysis, a plate of size 1 × 1 m, has been used. The plate examined by applying the Kirchhoff plate theory, while FEM was performed by using the Gaussian numerical integration by the quadrilateral element based on the standard matrix of stiffness formulation. The plate discretised in 20 × 20 equal sized elements. The isotropic and linearly elastic material was considered, with the value of E = 200 MPa and Poisson's ratio ν = 0.3. Finite element method (FEM) implemented through a MATLAB-based code performed in MATLAB 2025a.

ANSYS simulations were conducted in ANSYS Workbench, using the program controlled Shell 181 element type that support transverse displacement of a plate. The same geometric and material parameters were applied while performing simulations in ANSYS to ensure consistency

in comparison. The mesh was refined to achieve an element edge length of approximately 0.05 m, corresponding to a configuration of 400-element and 441 nodes.

Comparative analyses were performed for both simply supported and clamped boundary conditions under uniform loading. The results obtained from the proposed H-RBF Method were compared with those derived from Timoshenko's analytical solution, FEM (MATLAB-based), and ANSYS simulations. The outcomes, summarised in Table 1, demonstrate a strong agreement between the present method and the reference solutions.

Notably, the H-RBF Method achieved comparable accuracy at a 7 × 7 grid, while the results converged at considerably high grid size 20 × 20 in conventional FEM approach and ANSYS simulation to attain a similar level of precision.

The overall deviation for % error is also calculated for present method and the results of Timoshenko and the deviation lies in a range up to 0.99%. 0.2 to 0.99% deviation is observed in the case of Simple Supported boundary condition while closer to zero deviation is observed in clamped boundary condition depicts the numerical stability and consistency of the method. Such a very small deviation demonstrates the computational efficiency and robustness of the proposed method in comparison to the standard analytical method under both boundary conditions.

Further corroboration was achieved for anisotropic plate using the classic analytical solution framework developed by Ashton and Whitney [29], which is well-established for analysing anisotropic laminated plates subjected to a uniformly distributed load. Two boundary conditions, simple supported and clamped edges were employed for the study and their mathematical model is represented in Equation 16 and 17. Results were generated for various aspect ratios; the load and material properties were maintained uniform to ensure consistency.

Simple supported boundary condition

$$w = 16 \sum_{m=1}^{\infty} \sum_{n=1}^{\infty} \frac{qa^4b^4}{\pi^6 mn(D_{11}m^4b^4 + 2(D_{12} + 2D_{66})m^2n^2a^2b^2 + D_{22}n^4a^4)} \quad (16)$$

Clamped boundary condition

$$w = 0.00348 \frac{qa^4b^4}{D_{11}b^4 + 0.6047(D_{12} + 2D_{66})a^2b^2 + D_{22}a^4} \quad (17)$$

Tables 2 and 3 reveal the comparison of the proposed method against the classical solution shows an excellent agreement, confirming the methodological accuracy of the current approach in modelling the transverse bending of anisotropic plates.

Influence of material anisotropy

To examine the sensitivity of the model to material anisotropy, the plate was analysed with varying stiffness ratios (E_1/E_2 = 10, 20, 30, and 40) while maintaining G_{12}/E_2 = 0.5 and ν_{12} = 0.3. A computational approach based on the finite difference method (FDM), as proposed by K. Chandrashekhara [30], was used to validate the dimensionless displacement of anisotropic plates generated using the present method. The analysis

Table 2. The effect of aspect ratio (a/b) on displacement of plate for simple supported boundary condition E1/E2 = 14; G12/E2=0.5; v12=0.3

a/b	Ashton and Whitney W	H-RBF w
1.0	0.0117	0.01172
2.0	0.0157	0.01568
3.0	0.0163	0.01629
4.0	0.0165	0.01648
5.0	0.0165	0.01649
6.0	0.0166	0.01662
7.0	0.0166	0.01663
8.0	0.0166	0.01666
9.0	0.0166	0.01668

Table 1. Comparison of results for the plate subjected to transverse loading under different aspect ratios (a/b) and B.C.

Aspect ratio (a/b)	Boundary condition	Timoshenko [16]	FEM MATLAB code	FEA ANSYS simulation	Present method
		Maximum displacement, *w*			
1	S-S-S-S	0.00406	0.00405	0.00443	0.00410
	C-C-C-C	0.00126	0.00126	0.00137	0.00126
2	S-S-S-S	0.01013	0.01012	0.01103	0.01011
	C-C-C-C	0.00254	0.00252	0.00274	0.00254

Table 3. The effect of aspect ratio (a/b) on displacement of plate for Clamped boundary condition E1/E2 = 14; G12/E2=0.5; v12=0.3

a/b	Ashton and Whitney w	H-RBF w
1.0	0.00269	0.00270
2.0	0.00320	0.00325
3.0	0.00339	0.00338
4.0	0.00340	0.00342
5.0	0.00341	0.00344
6.0	0.00341	0.00345
7.0	0.00342	0.00347
8.0	0.00342	0.00346
9.0	0.00342	0.00348

considered both simple supported and clamped boundary conditions, with results presented in tabular and graphical forms. Tables 4 and 5 highlight the mechanical response of the plate under different aspect ratios and stiffness configurations.

The investigation of dimensionless displacement in anisotropic plates reveals significant variations in structural behaviour under different boundary conditions and stiffness ratios. For simple supported configurations, result shown in Figures 2 and 3 demonstrate a consistent reduction in dimensionless displacement as the stiffness ratio (E_1/E_2) increases from 10 to 40. This trend indicates enhanced structural resistance to deformation with higher material anisotropy. Ultimately, the displacement value approaches a virtually asymptotic value of approximately 0.0138, which may indicate a stabilisation of the mechanical response beyond some geometric proportions (aspect ratio a/b).

In clamped boundary conditions, similar patterns emerge but with notable differences in magnitude. The constrained edges result shown in Figures 4 and 5 represents substantially lower displacement values, converging near 0.00415 at higher aspect ratios.

Table 4. The effect of aspect ratio (a/b) and stiffness ratio on displacement of plate for simple supported boundary condition

E1/E2	10		20		30		40	
a/b	FDM	H-RBF	FDM	H-RBF	FDM	H-RBF	FDM	H-RBF
1.0	0.0024	0.00251	0.0023	0.00231	0.0022	0.00221	0.0021	0.00214
2.0	0.0100	0.01021	0.0104	0.01049	0.0107	0.01074	0.0108	0.01083
3.0	0.0129	0.01311	0.0134	0.01342	0.0137	0.01366	0.0139	0.01396
4.0	0.0136	0.01371	0.0139	0.01389	0.0141	0.01413	0.0142	0.01423
5.0	0.0137	0.01381	0.0139	0.01391	0.0140	0.01407	0.0141	0.01414
6.0	0.0137	0.01381	0.0138	0.01393	0.0139	0.01397	0.0139	0.01343
7.0	0.0137	0.01383	0.0138	0.01394	0.0138	0.01395	0.0138	0.01392
8.0	0.0137	0.01384	0.0137	0.01386	0.0138	0.01393	0.0138	0.01386
∞	0.0137	0.01385	0.0137	0.01381	0.0137	0.01382	0.0137	0.01383

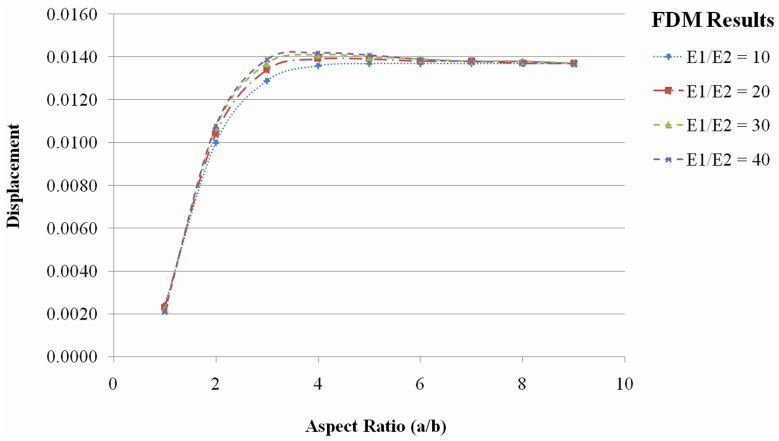

Figure 2. Displacement behaviour of for simple supported plate under the effect of aspect ratio (a/b) and stiffness ratio using the FDM method

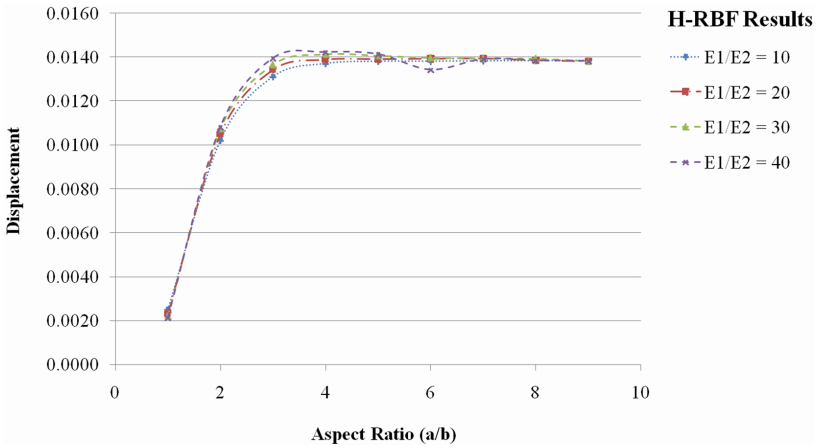

Figure 3. Displacement behaviour of for simple supported plate under the effect of aspect ratio (a/b) and stiffness ratio using the H-RBF method

Table 5. The effect of aspect ratio (a/b) and stiffness ratio on displacement of plate for clamped boundary condition

E1/E2	10		20		30		40	
a/b	FDM	H-RBF	FDM	H-RBF	FDM	H-RBF	FDM	H-RBF
	x 10^{-4}	x 10^{-4}	x 10^{-4}	x 10^{-4}	x 10^{-4}	x 10^{-4}	x 10^{-4}	x 10^{-4}
1.0	8.21	8.19	7.03	7.03	6.59	6.62	6.36	6.40
2.0	34.00	33.48	33.00	32.98	33.00	32.98	33.00	32.98
3.0	39.00	40.02	40.00	40.48	40.00	41.02	40.00	41.03
4.0	39.00	40.99	40.00	41.87	40.00	41.91	40.00	42.02
5.0	39.00	41.49	39.00	41.49	39.00	41.84	40.00	41.97
6.0	39.00	41.50	39.00	41.50	39.00	41.65	39.00	41.78
∞	39.00	41.50	39.00	41.50	39.00	41.54	39.00	41.59

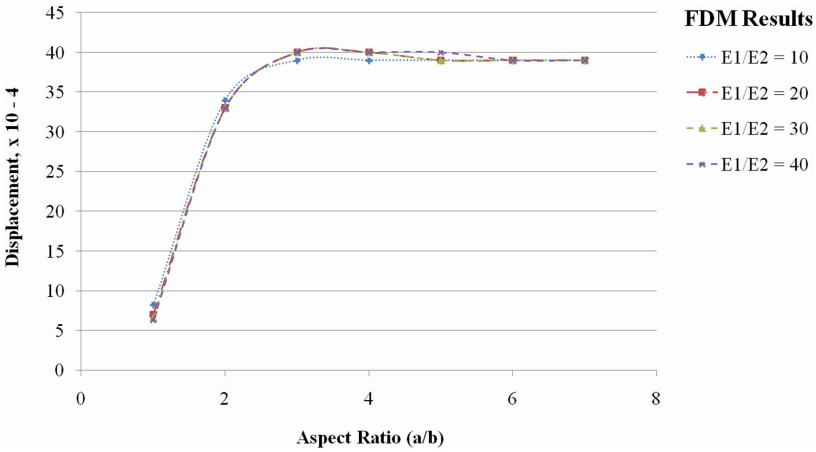

Figure 4. Displacement behaviour of for clamped plate under the effect of aspect ratio (a/b) and stiffness ratio using the FDM method

Comparative analysis shows that while both boundary conditions exhibit decreasing displacement with increasing stiffness ratios and the results are in very close agreement with the results of the FDM method. However, in both boundary conditions, variations in stiffness ratio do not influence dimensionless displacement with change in the aspect ratio. Particularly in square plates (a/b ≈ 1), the influence of material anisotropy appears most significant, gradually diminishing as the aspect ratio increases.

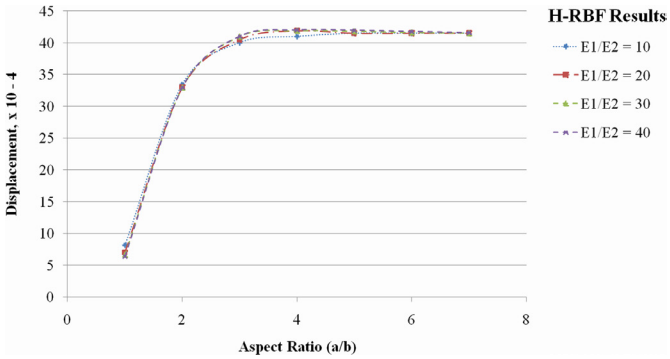

Figure 5. Displacement behaviour of for clamped plate under the effect of aspect ratio (a/b) and stiffness ratio using the H-RBF method

CONCLUSIONS

The proposed H-RBF method has been successfully validated against established classical plate theory, numerical, and computational models. The analysis across a variety of stiffness ratios, aspect ratios and boundary conditions shows confidence in the accuracy of the method and its use in both anisotropic and Isotropic plate analysis.

The present study emphasised the importance of the material anisotropy upon displacement behaviour, especially for the simple supported and clamped boundary conditions. The stiffness ratio has an effect on displacement behaviour such that higher stiffness ratios lead to lesser displacement; however, its effect tends to stabilise above certain geometric ratios. The behaviour observed across both boundary conditions further confirms convergence of results; therefore, this method predictive capability provides confidence on results, especially for large aspect ratios.

In conclusion, the proposed computational H-RBF method provided an effective and efficient tool for simulating the response of isotropic and anisotropic plates subjected to transverse loading. The framework replicated previously established results and captured changes in response from the different boundary conditions. Therefore, this H-RBF method can be a reliable tool for future studies into structural behaviour and composite material research.

REFERENCES

1. An D., Ni Z., Xu D., and Li R., New straightforward benchmark solutions for bending and free vibration of clamped anisotropic rectangular thin plates, Journal of Vibration and Acoustics, Dec. 2021; 144: 3, https://doi.org/10.1115/1.4053090
2. Leng B., Xu H., Yan Y., Wang K., Yang G., and Meng Y., An analytical solution for the bending of anisotropic rectangular thin plates with elastic rotation supports, Buildings, Mar. 2024; 14(3): 756, https://doi.org/10.3390/buildings14030756
3. Xu Y. and Wu Z., Exact solutions for rectangular anisotropic plates with four clamped edges, Mechanics of Advanced Materials and Structures, Nov. 2020; 29(12): 1756–1768, https://doi.org/10.1080/15376494.2020.1838007
4. Maji A. and Mahato P. K., Development and applications of shear deformation theories for laminated composite plates: An overview, Journal of Thermoplastic Composite Materials, June 2020; 35(12): 2576–2619, https://doi.org/10.1177/0892705720930765
5. Paiva W. P., Sollero P., and Albuquerque E. L., Dynamics of thin anisotropic plates, International Conference: BeTeq, Jul. 2004.
6. David Müzel S., Bonhin E. P., Guimarães N. M., and Guidi E. S., Application of the Finite Element Method in the Analysis of Composite Materials: A Review, Polymers, Apr. 2020; 12(4): 818. https://doi.org/10.3390/polym12040818
7. Brebbia C. A. and Dominguez J., The boundary element method for structural problems, in Boundary Elements: an introductory course, 2nd ed.WIT Press, 2001. https://www.witpress.com/books/978-1-85312-349-8
8. John Wiley and Sons, Inc, On a mixed-hybrid finite element method for anisotropic plate bending problems - Publications of the IAS Fellows. Available: https://repository.ias.ac.in/122949
9. Chen Y. T., Li C., Yao L. Q., and Cao Y., A hybrid RBF collocation method and its application in the elastostatic symmetric problems, Symmetry, Jul. 2022; 14(7): 1476, https://doi.org/10.3390/sym14071476
10. Kamal R., Kamran N., Alzahrani S. M., and Alzahrani T., A hybrid local radial basis function method for the numerical modeling of mixed diffusion

and Wave-Diffusion equations of fractional order using Caputo's derivatives, Fractal and Fractional, May 2023; 7(5): 381, https://doi.org/10.3390/fractalfract7050381

11. Qiu L., Wang F., Gu Y., and Qin Q., Modified space-time radial basis function collocation method for long-time simulation of transient heat conduction in3Danisotropic composite materials, International Journal for Numerical Methods in Engineering, Jul. 2023; 124(21): 4639–4658, https://doi.org/10.1002/nme.7327
12. Carrera E., Theories and finite elements for multilayered, anisotropic, composite plates and shells, Archives of Computational Methods in Engineering, Jun. 2002; 9(2): 87–140, https://doi.org/10.1007/bf02736649
13. Ferreira A. J. M., Analysis of composite plates using a layerwise theory and multiquadrics discretization, Mechanics of Advanced Materials and Structures, Mar. 2005; 12(2): 99–112, https://doi.org/10.1080/15376490490493952
14. Liew K. M., Zhao X., and Ferreira A. J. M., A review of meshless methods for laminated and functionally graded plates and shells, Composite Structures, Feb. 2011; 93(8): 2031–2041, https://doi.org/10.1016/j.compstruct.2011.02.018
15. Roque C. M. and Grasa J., Geometrically nonlinear analysis of laminated composite plates using RBF-PS meshless method, Composite Structures, Mar. 2021; 267: 113830, https://doi.org/10.1016/j.compstruct.2021.113830
16. Fernandes S. C., Cuartero J., and Ferreira A. J. M., Using collocation with radial basis functions in a pseudospectral framework for a new layerwise shallow shell theory, Journal of Composites Science, Nov. 2024; 8(11): 448, https://doi.org/10.3390/jcs8110448
17. Senel C.B., Jeroen Van Beeck J., and Altinkaynak A. A. A., Solving PDEs with a Hybrid Radial Basis Function: Power-Generalized Multiquadric Kernel, Advances in Applied Mathematics and Mechanics, Jan. 2022; 14(5): 1161–1180, https://doi.org/10.4208/aamm.oa-2021-0215
18. Ku C.Y., Liu C.Y., Xiao J.-E., and Hsu S.-M., Multiquadrics without the shape parameter for solving partial differential equations, Symmetry, Nov. 2020; 12(11): 1813, https://doi.org/10.3390/sym12111813
19. Tóth B. and Düster A., h-Adaptive radial basis function finite difference method for linear elasticity problems, Computational Mechanics, Nov. 2022; 71(3): 433–452, https://doi.org/10.1007/s00466-022-02249-9
20. Fouaidi M., Jamal M., and Belouaggadia N., Nonlinear bending analysis of functionally graded porous beams using the multiquadric radial basis functions and a Taylor series-based continuation procedure, Composite Structures, Jul. 2020; 252: 112593, https://doi.org/10.1016/j.compstruct.2020.112593
21. Kalita K., Chakraborty S., Madhu S., Ramachandran M., and Gao X.-Z., Performance analysis of radial basis function metamodels for predictive modelling of laminated composites, Materials, Jun. 2021; 14(12): 3306, https://doi.org/10.3390/ma14123306
22. Nguyen N. T., Lo V. S., Nguyen D. K., and Truong T. T., A novel extended integrated radial basis functions meshfree method for crack analysis in plate problem, Engineering Analysis With Boundary Elements, Jan. 2024; 160: 201–212, https://doi.org/10.1016/j.enganabound.2023.12.022
23. Wen P. H. and Hon Y. C., Geometrically nonlinear analysis of Reissner-Mindlin plate by meshless computation, Computer Modeling in Engineering & Sciences, Oct. 2007; 21(3): 177–191, https://doi.org/10.3970/cmes.2007.021.177
24. Daxini S. D. and Prajapati J. M., A review on recent contribution of meshfree methods to structure and fracture mechanics applications, The Scientific World Journal, 2014; 2014: 1–13, Jan. https://doi.org/10.1155/2014/247172
25. Arora G., KiranBala N., Emadifar H., and Khademi M., A review of radial basis function with applications explored, Journal of the Egyptian Mathematical Society, Nov. 2023; 31(1), https://doi.org/10.1186/s42787-023-00164-3
26. Misra R. K., Sandeep K., and Misra A., Analysis of anisotropic plate using multiquadric radial basis function, Engineering Analysis With Boundary Elements, Sep. 2006; 31(1): 28–34, https://doi.org/10.1016/j.enganabound.2006.06.003
27. Kumar M., Jha A. K., Bhagoria Y., and Gupta P., A review to explore different meshless methods in various Structural problems, IOP Conference Series Materials Science and Engineering, Apr. 2021; 1116(1): 012119, https://doi.org/10.1088/1757-899x/1116/1/012119
28. Timoshenko S. and Woinowsky Krieger S., Pure bending of plates & bending of anisotropic plates, in Theory of Plates and Shells, 2nd ed.McGRAW-HILL BOOK COMPANY. Available:https://structures.dhu.edu.cn/_upload/article/files/c2/53/6997426d-46cb8f09fcd5d26175e2/c2f8856e-aedf-4149-8170-8b1127b9afb6.pdf
29. Ashton J. E. and Whitney J. M., Equations of Laminated Anisotropic Plate, in Theory of Laminated Plates, vol. 4.
30. Chandrashekhara K., Plates and shells, in *Theory of Plates*, Hyderabad: University Press(India) Ltd, 2001.